Accessing One-Dimensional Chains of Halogenoindates(III) in Organic−Inorganic Hybrids

Magdalena Owczarek,* Minseong Lee, Vivien Zapf, Wanyi Nie, and Ryszard Jakubas

Read Online

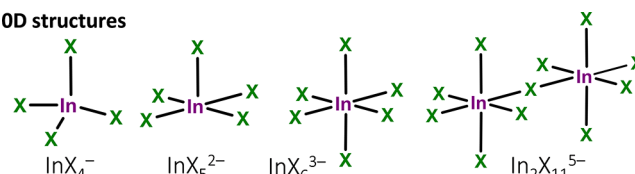ACCESS | Metrics & More | Article Recommendations | Supporting Information

ABSTRACT: Organic−inorganic hybrids of halogenoindates(III) are typically represented by one of the zero-dimensional units: InX_4^-, InX_5^{2-}, InX_6^{3-}, or $In_2X_{11}^{5-}$. Higher dimensional anionic forms, although not forbidden, have remained almost elusive. Here we report for the first time In^{3+}-based organic−inorganic hybrids, $(C_4H_5N_2S)_2InCl_5$ and $(C_4H_5N_2S)_2InBr_5$, with 1D anionic chains of *trans*-halide-bridged InX_6 octahedra whose formation is guided by 2-mercaptopyrimidinium cations ($C_4H_5N_2S^+$). The chains are characterized by the significant ease of deformation, which is reflected in the elongation of the bridging bonds or the displacement of In^{3+} ions. The materials show a robust band gap predominantly governed by $C_4H_5N_2S^+$ cations. Dielectric relaxation processes in $(C_4H_5N_2S)_2InBr_5$ arise from the cations' dynamics and suggest the ability of the brominated system to accommodate even larger cations. Our work represents a successful attempt to expand the structural diversity of halogenoindates(III) and opens a pathway to reach multifunctional 1D In^{3+}-based hybrids.

Organic−inorganic hybrids continue to gather significant attention due to their attractive properties for applications in photonics, optoelectronics, and energy technologies.[1,2] Materials particularly widely explored are organic−inorganic metal halides of groups 14 (Sn^{2+} and Pb^{2+}) and 15 (Sb^{3+} and Bi^{3+}) characterized by the high tunability of their optical and electronic properties achieved by either halide substitution or promotion to analogs with higher dimensional anionic structures (1D, 2D, or 3D).[3] In contrast, metal halides of group 13 (Ga^{3+} and In^{3+}) are rarely employed as a base of such hybrids presumably because of the low variety of anionic forms they offer; they are commonly encountered as 0D tetrahedral units, $(Ga, In)X_4^-$ ($X = Cl^-$, Br^-, I^-),[4,5] used often only to balance the charge of large organic systems.[6−8] In some cases, they have been found to contribute to order−disorder structural phase transitions.[9,10] 0D units with higher coordination numbers have been accessed only by In^{3+} (InX_5^{2-} ($X = Cl^-$, Br^-), InX_6^{3-} ($X = Cl^-$, Br^-, I^-), and $In_2X_{11}^{5-}$ ($X = Br^-$) (Scheme 1)) and have been found to play a key role in the nonlinear electrical and nonlinear optical properties of materials.[11−13]

Whereas the potential to form more complex anionic forms via the corner-sharing assembly of InX_6 octahedra in organic−inorganic hybrids became apparent with the publication of the dioctahedral $In_2Br_{11}^{5-}$ unit,[14] it was only recently that the first example of a higher dimensional form was obtained: a 1D chain of *cis*-connected octahedra ($\angle(X_{bridging}-M-X_{bridging}) \approx 90°$; (Scheme 1)).[15] The significance of this finding lies in the fact that, in general, 1D anionic forms determine the properties of materials more profoundly. For instance, 1D chains' high susceptibility for deformation in many cases leads to the appearance of desirable properties such as piezo- and ferroelectricity or second-harmonic generation.[16−20] An assembly of octahedral units into 1D structures strongly depends, however, on an organic cation incorporated into the system, specifically, its size, type (aromatic vs aliphatic), and proton-

Scheme 1. Anionic Structures of Halogenoindates(III) Observed in Organic−Inorganic Hybrids
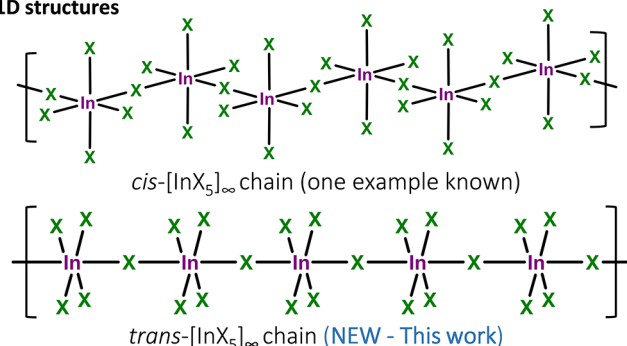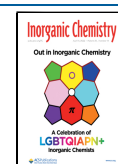

donating/accepting abilities defining the intermolecular interactions and hence driving the crystal packing. Whereas there are no specific rules for choosing a cation to obtain a target anionic form, some types of cations show a strong propensity to direct the formation of a particular anionic structure. Pyrimidine

derivatives, for instance, used with halogenoantimonates(III) and halogenobismuthates(III) tend to drive the latter toward rare 1D chains of *trans*-connected octahedra [$\angle(X_{bridging}-M-X_{bridging}) \approx 180°$; $M = Bi^{3+}/Sb^{3+}$, $X = Cl^-$, Br^-].[16,21] In the effort to expand the family of anionic forms of In^{3+} halides, we decided to investigate whether a similar structural architecture can be formed out of halogenoindates(III).

In this work, we report two In^{3+}-based compounds (Figure 1a) with the 2-mercaptopyrimidinium cation, $(C_4H_5N_2S)_2InCl_5$

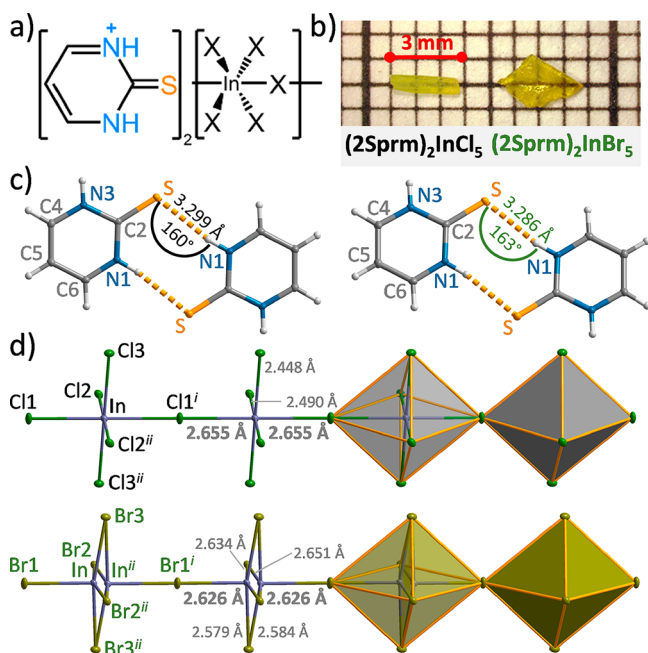**Figure 1.** (a) Structural formula of $(2Sprm)_2InX_5$ ($X = Cl^-$, Br^-) compounds. (b) Photographs of the crystals. (c) Dimers of 2Sprm$^+$ cations with atom numbering scheme and geometrical parameters of hydrogen bonds. Left: $(2Sprm)_2InCl_5$; Right: $(2Sprm)_2InBr_5$. (d) *trans*-$[InX_5]_\infty$ anionic chains with atom numbering scheme and In−X distances. Symmetry codes: (*i*) $x-1$, y, z; (*ii*) $-x$, $-y+1$, $-z+1$. Thermal ellipsoids of non-hydrogen atoms in panels c and d are shown at the 50% probability level.

(abbrev. $(2Sprm)_2InCl_5$) and $(C_4H_5N_2S)_2InBr_5$ (abbrev. $(2Sprm)_2InBr_5$), with robust band gaps of $\sim$2.58 (direct nature) or $\sim$2.47 eV (indirect nature). The compounds are unique in terms of their anionic structure; it is composed of 1D chains of *trans*-halide-sharing octahedra that have not yet been observed in the organic−inorganic hybrids of halogenoindates-(III). Because of the axial symmetrical deformation of the octahedra, the chains remain apolar and drive the centrosymmetric packing ($P2_1/n$ space group). The significant ease of deformation, however, is a promising indication of halogenoindates(III)' potential to also produce noncentrosymmetric structures that could induce nonlinear electrical and optical properties. To this end, we anticipate that the presented results will serve as a first step in establishing a pathway to reach multifunctional 1D organic−inorganic hybrids based on halogenoindates(III).

Dark yellow crystals of $(2Sprm)_2InCl_5$ and $(2Sprm)_2InBr_5$ (Figure 1b) were grown from an aqueous acidic solution (HCl and HBr, respectively) of stoichiometric amounts of 2-mercaptopyrimidine and In_2O_3. The composition of the crystals was confirmed by elemental analysis and single-crystal X-ray diffraction studies. X-ray powder diffraction (Figure S4)

confirmed the presence of one phase. The structural stability of the materials was investigated using differential scanning calorimetry; no solid-state phase transitions were detected between 125 K and the melting points of the materials (Figures S2 and S3).

$(2Sprm)_2InCl_5$ and $(2Sprm)_2InBr_5$ are isomorphous with each other and also with the published $(2Sprm)_2BiCl_5$, $(2Sprm)_2BiBr_5$, $(2Sprm)_2SbCl_5$, and $(2Sprm)_2SbBr_5$.[16] Both compounds crystallize in the centrosymmetric $P2_1/n$ space group with two formula units per unit cell and similar cell dimensions: $a = 5.310(2)$, $b = 14.886(3)$, $c = 10.356(3)$ Å, $\beta = 103.87(3)°$ for $(2Sprm)_2InCl_5$ and $a = 5.789(2)$, $b = 15.115(3)$, $c = 10.342(3)$ Å, $\beta = 105.83(3)°$ for $(2Sprm)_2InBr_5$ (100 K data collection; Table S1). In both cases, 2-mercaptopyrimidine cation $(2Sprm)^+$ adopts its thione tautomeric form (Figure 1c) and creates a dimer that is typical for pyrimidinium derivatives,[16] located around a symmetry center, with another molecule of its type via N1−H1···S hydrogen bonds (3.2994(14) Å and 160.1° and 3.286(4) Å and 163.2° for $(2Sprm)_2InCl_5$ and $(2Sprm)_2InBr_5$, respectively).

The anionic structures are composed of 1D chains of octahedral InX_6 units ($X = Cl$ or Br; Figure 1d). The units are connected in *trans* configuration; X1 ligands located on the opposite sites of the octahedron are shared between the units, resulting in the formation of *trans*-$[InX_5]_\infty$ chains. Despite the materials being isomorphous, *trans*-$[InCl_5]_\infty$ and *trans*-$[InBr_5]_\infty$ chains differ in the octahedral deformation arising from the corner-sharing assembly. In the case of $(2Sprm)_2InCl_5$, the axial In−Cl1 bond becomes significantly elongated (2.6550(10) Å) relative to the equatorial In−Cl distances (2.4481(8) to 2.4900(6) Å), a tendency also observed in isolated $InCl_6^{3-}$ units where the elongation is caused by strong intermolecular interactions.[22] $(2Sprm)_2InBr_5$, on the contrary, preserves the axial In−Br1 distance (2.6256(10) Å) in a similar range as the equatorial In−Br distances (2.5788(11) to 2.6510(10) Å). Instead, the deformation is located around the center of the octahedron, where In^{3+} is displaced ($\sim$0.270 Å) along the chain's direction from the special position, leading to a disorder of the metal ion between two positions with 0.5 occupancy each and causing a significant deviation of Br−In−Br angles from the regular 180 and 90° (Table S2).

The packing of anionic and cationic moieties in the crystals of $(2Sprm)_2InCl_5$ and $(2Sprm)_2InBr_5$ resembles a chessboard arrangement (Figure 2a) when viewed along the inorganic chains, with the chains separated from each other by the stacks of 2Sprm$^+$ cations. In Figure 2, $(2Sprm)_2InCl_5$ is used as a representative of the two isomorphous compounds. The chain−chain distance between subsequent anionic units along the *b* axis, 14.886 Å for $(2Sprm)_2InCl_5$ and 15.115 Å for $(2Sprm)_2InBr_5$, determines the size of the voids occupied by the organic units and seems to impact the dynamics of these units when an external ac electric field is applied. (See as follows.) 2Sprm$^+$ dimers position themselves in the voids at a $\sim$45° angle relative to the chains' main axis (Figure 2b) and form hydrogen bonds with the closest *trans*-$[InX_5]_\infty$ chains to stabilize their position: N3−H3···Cl2 of 3.1547(16) Å and 169.7° and N3−H3···Br2 of 3.356(4) Å and 167.4° for $(2Sprm)_2InCl_5$ and $(2Sprm)_2InBr_5$, respectively.

Guiding the formation of rare *trans*-$[MX_5]$ chains in the family of not only halogenoindates(III) but also halogenoantimonates(III) and halogenobismuthates(III)[16] points to the 2Sprm$^+$ cations' peculiar ability to selectively promote this specific anionic arrangement. As the extended
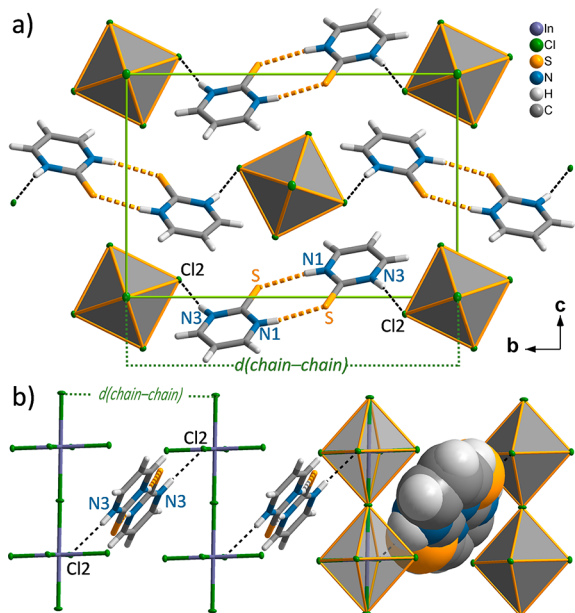
Figure 2. (a) Unit-cell packing of $(2Sprm)_2InCl_5$ along the a axis. (b) Position of $2Sprm^+$ dimers relative to the anionic chains.

analysis of Sb^{3+}/Bi^{3+} structures concluded, this ability is attributed to the void-matching size of $2Sprm^+$ dimers (4.4 Å × 10.6 Å) and the advantageous position of the proton-donating groups that can easily form highly directional (∼170°) contacts with the chains. In terms of designing new In^{3+}-based hybrids, these geometrical parameters might serve as a gateway to expanding the family of 1D halogenoindates(III).

By using dielectric spectroscopy, we probed dynamics of molecules in the systems. Only in the case of $(2Sprm)_2InBr_5$ (larger chain−chain distance) were relaxation processes observed: a weak one between 70 and 140 K and a stronger one below 70 K (Figure 3). Although the involvement of anionic chains in the processes cannot be fully excluded,[17,23,24] such low-frequency dynamics is characteristic of librational motions of larger moieties.[25,26] It is suspected then that the processes arise from a field-induced deformation of the nonpolar organic dimer causing the appearance of a nonzero electric dipole. From the peaks of the dielectric losses, the macroscopic relaxation time was estimated to be in the range of 1.37×10^{-7} to 4.43×10^{-6} s. The activation energy values, calculated from the Arrhenius

relation $\tau = C \exp\left(\frac{E_a}{kT}\right)$ (Figure S6), were determined to be 3 ($T < 70$ K) and 13 kJ/mol ($70 < T < 140$ K), which are significantly lower than 33 and 58 kJ/mol of the published isomorphous $(2Sprm)_2BiCl_5$.[16] Whereas both systems are characterized by similar chain−chain distances (15.108(3) vs 15.082(5) Å) and N−H···S contacts forming the $2Sprm^+$ dimer (3.283(3) Å and 163.2° vs 3.2852(17) Å and 164°), the difference in E_a presumably stems from the different strengths of hydrogen bonds stabilizing the organic dimers between the inorganic chains (N−H···Br 3.356(4) Å and 167.4° in $(2Sprm)_2InBr_5$ vs N−H···Cl 3.203(2) Å and 168° in $(2Sprm)_2BiCl_5$).[16] This implies the different characters and anisotropies of the dipole−dipole interactions that impact the dielectric response of the two compounds. A similar distribution of E_a values has been observed in other structurally isomorphous organic−inorganic hybrids.[27,28]

The optical properties of the crystals were investigated by using UV−vis absorbance spectroscopy. Suggested already by the color of the crystals (Figure 1b), $(2Sprm)_2InCl_5$ and $(2Sprm)_2InBr_5$ absorb light of a similar wavelength from the visible region. A steep absorption edge is observed at ∼490 nm for both compounds (Figure 4), and thus the band gaps determined from the Tauc plot are almost identical: 2.58 vs 2.57 eV for a direct-nature gap and 2.47 vs 2.46 eV for an indirect-nature gap (insets in Figure 4). In comparison with other organic−inorganic hybrids where the tunability of optical properties is achieved by, for instance, halide doping, the unchanged position of the absorption band upon halide substitution in $(2Sprm)_2InCl_5$ and $(2Sprm)_2InBr_5$ materials strongly suggests that the halides might not dominate the band edge states, leaving the organic component of the compounds, $2Sprm^+$ cations, as the main contributors. Although the fact that 2Sprm itself, the starting material, is also a bright yellow solid (Figure S1) with a ∼2.68 eV band gap (direct-nature; 2.56 eV indirect; Figure S5) might confirm this possibility, rigorous density functional theory (DFT) calculations are needed to obtain more details of the band gap and to unequivocally determine its nature.

In summary, we report the synthesis and structural characterization of the first In^{3+}-based organic−inorganic hybrids, $(2Sprm)_2InCl_5$ and $(2Sprm)_2InBr_5$, with unprecedented 1D chains of *trans*-connected InX_6 octahedra. The formation of the chains is supported by $2Sprm^+$ cations specifically selected on the basis of their strong tendency to form dimers whose size and
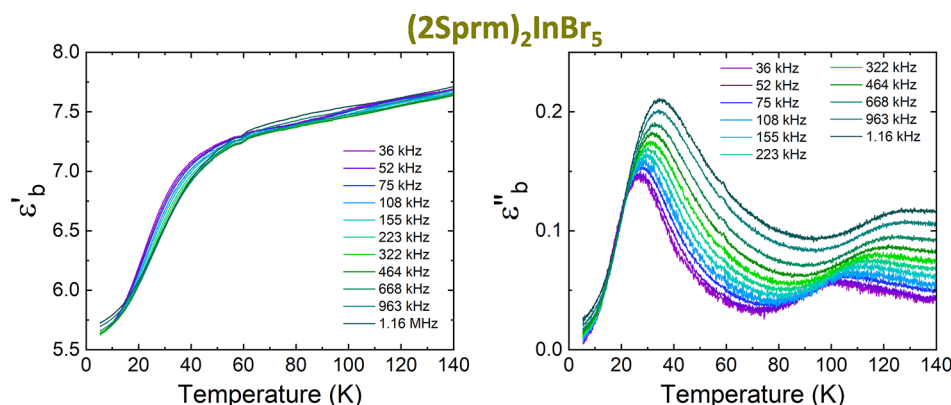

Figure 3. Temperature dependence of real (ε') and imaginary (ε'') parts of the complex electric permittivity of $(2Sprm)_2InBr_5$ collected on cooling along the b axis.

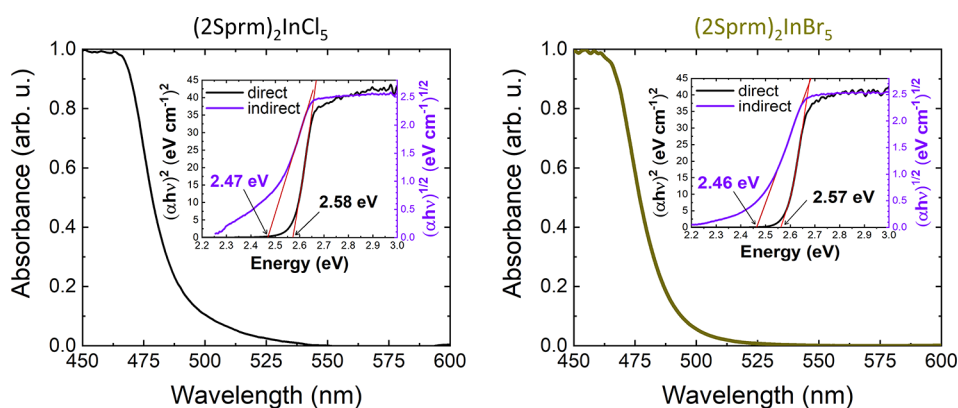**Figure 4.** Normalized absorbance spectra of $(2Sprm)_2InCl_5$ (left) and $(2Sprm)_2InBr_5$ (right). Insets: Tauc plots with the estimated band gaps for direct- and indirect-nature gaps.

proton-donating abilities are accommodated particularly well in the *trans*-$[MX_5]$ chains setting. This indicates that 1D forms of halogenoindates(III) are accessible when specific geometrical requirements are met by organic cations, although some flexibility in cations' size can be assumed based on the observed dielectric relaxation processes in $(2Sprm)_2InBr_5$. We also note that the $2Sprm^+$ cation is suspected to govern the band gaps of the materials. Whereas the compounds are isomorphous, we found fundamental differences in the chains' adjustment to deformation caused by *trans*-halide sharing: In $(2Sprm)_2InCl_5$, the elongation of the bridging bonds is preferred over the dislocation of In^{3+} from the octahedron center observed in $(2Sprm)_2InBr_5$. In any case, such susceptibility for deformation is a promising feature in many contexts, for example, piezo- and ferroelectricity or the second-harmonic generation of light, and can provide an appealing basis for the further development of 1D halogenoindates(III) showing a range of interesting nonlinear optical and electrical properties.

■ ASSOCIATED CONTENT

SI Supporting Information

The Supporting Information is available free of charge at https://pubs.acs.org/doi/10.1021/acs.inorgchem.2c00374.

> Synthesis and crystal growth description, material characterization, instruments, thermal analysis, crystal data and structure refinement parameters, selected bond lengths and angles, hydrogen-bond parameters, PXRD spectra, additional UV−vis spectra, and dielectric data (PDF)

Accession Codes

CCDC 2132471−2132472 contain the supplementary crystallographic data for this paper. These data can be obtained free of charge via www.ccdc.cam.ac.uk/data_request/cif, or by emailing data_request@ccdc.cam.ac.uk, or by contacting The Cambridge Crystallographic Data Centre, 12 Union Road, Cambridge CB2 1EZ, UK; fax: +44 1223 336033.

■ AUTHOR INFORMATION

Corresponding Author

Magdalena Owczarek − *Materials and Applications Division, Center for Integrated Nanotechnologies, Los Alamos National Laboratory, Los Alamos, New Mexico 87545, United States;* orcid.org/0000-0001-8747-1857; Email: magdalena@lanl.gov

Authors

Minseong Lee − *National High Magnetic Field Lab, Los Alamos National Laboratory, Los Alamos, New Mexico 87545, United States*

Vivien Zapf − *National High Magnetic Field Lab, Los Alamos National Laboratory, Los Alamos, New Mexico 87545, United States;* orcid.org/0000-0002-8375-4515

Wanyi Nie − *Materials and Applications Division, Center for Integrated Nanotechnologies, Los Alamos National Laboratory, Los Alamos, New Mexico 87545, United States;* orcid.org/0000-0002-5909-3155

Ryszard Jakubas − *Faculty of Chemistry, University of Wroclaw, 50-383 Wroclaw, Poland;* orcid.org/0000-0002-2464-8309

Complete contact information is available at:
https://pubs.acs.org/10.1021/acs.inorgchem.2c00374

Notes

The authors declare no competing financial interest.

■ ACKNOWLEDGMENTS

■ REFERENCES

(1) Correa-Baena, J.-P.; Saliba, M.; Buonassisi, T.; Grätzel, M.; Abate, A.; Tress, W.; Hagfeldt, A. Promises and Challenges of Perovskite Solar Cells. *Science* **2017**, *358* (6364), 739−744.

(2) Zhang, W.; Eperon, G. E.; Snaith, H. J. Metal Halide Perovskites for Energy Applications. *Nature Energy* **2016**, *1* (6), 16048.

(3) Jakubas, R.; Rok, M.; Mencel, K.; Bator, G.; Piecha-Bisiorek, A. Correlation Between Crystal Structures and Polar (Ferroelectric)

Properties of Hybrids of Haloantimonates(III) and Halobismuthates-(III). *Inorganic Chemistry Frontiers* **2020**, *7* (10), 2107−2128.

(4) Fattal, H.; Creason, T. D.; Delzer, C. J.; Yangui, A.; Hayward, J. P.; Ross, B. J.; Du, M.-H.; Glatzhofer, D. T.; Saparov, B. Zero-Dimensional Hybrid Organic−Inorganic Indium Bromide with Blue Emission. *Inorg. Chem.* **2021**, *60* (2), 1045−1054.

(5) Zhou, L.; Liao, J.-F.; Huang, Z.-G.; Wei, J.-H.; Wang, X.-D.; Chen, H.-Y.; Kuang, D.-B. Intrinsic Self-Trapped Emission in 0D Lead-Free $(C_4H_{14}N_2)_2In_2Br_{10}$ Single Crystal. *Angew. Chem., Int. Ed.* **2019**, *58* (43), 15435−15440.

(6) Klaui, W.; Peters, W.; Liedtke, N.; Trofimenko, S.; Rheingold, A. L.; Sommer, R. D. Nitrogen Tripod Ligand/Oxygen Tripod Ligand Indium(III) Complexes: The First Structurally Characterized Trofimenko−Kläui Complex $[\eta^5-(C_5H_5)Co\{P(OCH_3)_2(O)\}_3InHB(pz)_3]$-$[InCl_4]$ (pz = pyrazol-1-yl). *Eur. J. Inorg. Chem.* **2001**, *2001* (3), 693−699.

(7) Plommer, H.; Murphy, J. N.; Dawe, L. N.; Kerton, F. M. Morpholine-Stabilized Cationic Aluminum Complexes and Their Reactivity in Ring-Opening Polymerization of ε-Caprolactone. *Inorg. Chem.* **2019**, *58* (8), 5253−5264.

(8) Presly, O. C.; Green, M.; Jeffery, J. C.; Leiner, E.; Murray, M.; Russell, C. A.; Scheer, M.; Vogel, U. The Surprising and Stereoselective Formation of P_2C_{10} Cages by the Reduction of Cp*PCl$_2$. *Chem. Commun.* **2006**, No. 43, 4542−4544.

(9) Li, M.; Xu, G.-C.; Xin, W.-B.; Zhang, Y.-Q. A In(III)-Based Organic-Inorganic Hybrid Compound: $(C_4H_7N_2)_4[InBr_6][InBr_4]\cdot$2H$_2$O with a Two-Step Phase Transition and Switchable Dielectric Property. *Polyhedron* **2020**, *189*, 114725.

(10) Zhang, Y.-Q.; Xu, G.-C.; Li, M. Two In-Based Organic−Inorganic Hybrid Compounds with Reversible Phase Transition Derived from the Order−Disorder Changes of Cations or Anions. *Dalton Transactions* **2021**, *50* (35), 12287−12291.

(11) Chen, D.; Hao, S.; Fan, L.; Guo, Y.; Yao, J.; Wolverton, C.; Kanatzidis, M. G.; Zhao, J.; Liu, Q. Broad Photoluminescence and Second-Harmonic Generation in the Noncentrosymmetric Organic−Inorganic Hybrid Halide $(C_6H_5(CH_2)_4NH_3)_4MX_7\cdot$H$_2$O (M = Bi, In, X = Br or I). *Chem. Mater.* **2021**, *33* (20), 8106−8111.

(12) Xin, W.-B.; Xu, G.-C.; Li, M. Synthesis and Characterization of a New Organic−Inorganic Hybrid Ferroelectric: $(C_4H_{10}N)_6[InBr_6]$-$[InBr_4]_3\cdot$H$_2$O. *Dalton Transactions* **2019**, *48* (46), 17402−17407.

(13) Zhang, Y.-Q.; Xu, G.-C.; Luo, Y. $C_2H_5NH_3)_3[InBr_6]$: an Indium(III) Organic−Inorganic Hybrid Phase Transition Compound Exhibiting a Switchable Dielectric Response. *New J. Chem.* **2021**, *45* (43), 20140−20143.

(14) Iwakiri, T.; Terao, H.; Lork, E.; Gesing, T. M.; Ishihara, H. X-ray and NQR Studies of Bromoindate(III) Complexes: $[C_2H_5NH_3]_4InBr_7$, $[C(NH_2)_3]_3InBr_6$, and $[H_3NCH_2C(CH_3)_2CH_2NH_3]InBr_5$. *Zeitschrift für Naturforschung B* **2017**, *72* (2), 141−151.

(15) Li, M.; Xu, G.-C.; Zhang, Y.-Q.; Xin, W.-B. Phase Transition, Dielectric Switching Property of an In(III)-Based Organic-Inorganic Hybrid Compound: $(C_5H_{16}N_2)InBr_5$. *J. Solid State Chem.* **2020**, *287*, 121329.

(16) Owczarek, M.; Szklarz, P.; Jakubas, R. Towards Ferroelectricity-Inducing Chains of Halogenoantimonates(III) and Halogenobismuthates(III). *RSC Adv.* **2021**, *11* (29), 17574−17586.

(17) Bi, W.; Leblanc, N.; Mercier, N.; Auban-Senzier, P.; Pasquier, C. Thermally Induced Bi(III) Lone Pair Stereoactivity: Ferroelectric Phase Transition and Semiconducting Properties of (MV)BiBr$_5$ (MV= Methylviologen). *Chem. Mater.* **2009**, *21* (18), 4099−4101.

(18) Owczarek, M.; Szklarz, P.; Jakubas, R.; Miniewicz, A. $[NH_2(C_2H_4)_2O]MX_5$: a New Family of Morpholinium Nonlinear Optical Materials among Halogenoantimonate(III) and Halogenobismuthate(III) Compounds. Structural Characterization, Dielectric and Piezoelectric Properties. *Dalton Transactions* **2012**, *41* (24), 7285−7294.

(19) Leblanc, N.; Mercier, N.; Zorina, L.; Simonov, S.; Auban-Senzier, P.; Pasquier, C. Large Spontaneous Polarization and Clear Hysteresis Loop of a Room-Temperature Hybrid Ferroelectric Based on Mixed-Halide $[BiI_3Cl_2]$ Polar Chains and Methylviologen Dication. *J. Am. Chem. Soc.* **2011**, *133* (38), 14924−14927.

(20) Piecha-Bisiorek, A.; Gągor, A.; Jakubas, R.; Ciżman, A.; Janicki, R.; Medycki, W. Ferroelectricity in Bis(ethylammonium) Pentachlorobismuthate(III): Synthesis, Structure, Polar and Spectroscopic Properties. *Inorganic Chemistry Frontiers* **2017**, *4* (8), 1281−1286.

(21) Ozturk, I. I.; Hadjikakou, S. K.; Hadjiliadis, N.; Kourkoumelis, N.; Kubicki, M.; Tasiopoulos, A. J.; Scleiman, H.; Barsan, M. M.; Butler, I. S.; Balzarini, J. New Antimony(III) Bromide Complexes with Thioamides: Synthesis, Characterization, and Cytostatic Properties. *Inorg. Chem.* **2009**, *48* (5), 2233−2245.

(22) Bouacida, S.; Belhouas, R.; Fantazi, B.; Boudaren, C.; Roisnel, T. Tris(piperazine-1,4-diium) Bis[hexachloridoindate(III)] Tetrahydrate. *Acta Crystallographica Section E* **2011**, *67* (4), m400−m401.

(23) Piecha, A.; Białońska, A.; Jakubas, R. Novel Organic−Inorganic Hybrid Ferroelectric: Bis(Imidazolium) Pentachloroantimonate(III), $(C_3N_2H_5)=SbCl_5$. *J. Mater. Chem.* **2012**, *22* (2), 333−336.

(24) Zhao, W.-P.; Shi, C.; Stroppa, A.; Di Sante, D.; Cimpoesu, F.; Zhang, W. Lone-Pair-Electron-Driven Ionic Displacements in a Ferroelectric Metal−Organic Hybrid. *Inorg. Chem.* **2016**, *55* (20), 10337−10342.

(25) Lu, Y.; Wang, Z.; Chen, H.-P.; Ge, J.-Z. High Temperature Structural Phase Transition and Dielectric Relaxation in an Organic−Inorganic Hybrid Compound: (4-methylpiperidinium)CdCl$_3$. *CrystEngComm* **2017**, *19* (14), 1896−1901.

(26) Yuan, X.-H.; Shao, X.-D.; Shi, C.; Zhang, W. Dielectric Transition and Relaxation in an Imidazolium-Based Organic-Inorganic Hybrid Crystal $(HIm)_6[(CdCl_4)(CdCl_6)]$. *Inorg. Chem. Commun.* **2016**, *67*, 35−39.

(27) Piecha, A.; Jakubas, R.; Kinzhybalo, V.; Lis, T. Structural and Dielectric Properties of Thiazolium Chlorobismuthate(III) and Chloroantimonate(III). *J. Mol. Struct.* **2008**, *887* (1), 194−200.

(28) Piecha, A.; Jakubas, R.; Kinzhybalo, V.; Medycki, W. Crystal Structure, Dielectric Properties and Molecular Motions of Molecules in Thiazolium Halometalates(III): $(C_3H_4NS)_6M_4Br_{18}\cdot$2H$_2$O (M = Sb, Bi). *J. Mol. Struct.* **2012**, *1013*, 55−60.